Scalar and Representative Models for Polarimetric SAR Data

Thanh-Hai Le, Ian McLoughlin, and Chan-Hua Vun

Abstract

This paper presents two novel scalar statistical models for the determinant of both partial and full polarimetric SAR (POLSAR) covariance matrices. Compared to other scalar statistical models for POLSAR, the proposed models are highly representative of the multi-dimensional data and consequently they lead to useful discrimination measures. The representative power of these multi-dimensional models is illustrated when they are collapsed into the special case of one-dimensional, the special-case statistical models then match perfectly with the traditionally used statistical models for SAR intensity. These theoretical models, together with their derived discrimination measures, are then validated against practically captured POLSAR data. These validated generic models are envisioned to form a bridge allowing the adaptation of many existing SAR data processing techniques for POLSAR data. For example, similar to the way that the intensity ratio is routinely used to evaluate SAR speckle filters, this paper describes how the determinant-ratio and its additive version, contrast, can be used to evaluate POLSAR speckle filters.

Index Terms

Polarimetric Synthetic aperture radar, Electromagnetic Modeling, Multidimensional signal processing

I. Introduction

In the past decades, the exponential growth in computational power has made the once overly-excessive computationaly-demanding SAR technology now become a feasible and preferred earth

Thanh-Hai Le and Chan-Hua Vun are with School of Computer Engineering, Nanyang Technological University, Singapore. Ian McLoughlin is with School of Information Science and Technology, University of Science and Technology of China.

Manuscript received ?, 2013; revised ?.

observation solution. As state-of-the-art technology, the SAR technique has been extended in a few directions, one of which is the polarimetric SAR. POLSAR is the natural extension from SAR exploiting the natural polarization property of Electro-Magnetic (EM) waves. Similar to the extension from black-and-white images to color photography, the polarimetric extension brought about the multi-channels POLSAR data as compared to the traditional one-channel SAR data.

While statistical models are important in understanding the stochastic nature of both SAR and POLSAR, in extending our understanding towards multi-dimensional POLSAR data, an important issue needs to be addressed. The trouble that the high dimensional data bring about is that there exists not one, as the intensity in the one-channel SAR, but many observables quantities in multi-channel POLSAR. While different statistical models have been developed for different POLSAR observables, for a statistical model to be useful, scalar discrimination measures need to be derived from it. Thus practical application for POLSAR data processing requires the dissimilarity measure to be scalar, consistent and preferably homoskedastic on one hand. On the other hand, the observable quantity being modelled needs to be naturally representative for the high dimensional POLSAR data.

In this paper, the determinant of the POLSAR covariance matrix is proposed as an observable quantity to study. Statistical models for this heteroskedastic POLSAR determinant and homoskedastic log-determinant, together with several discrimination measures, are then derived in section III. The representative power of this observable is demonstrated in section IV, where the multi-dimensional POLSAR data is collapsed into the traditional one-dimensional SAR scenario. Under this transformation, the determinant of the POLSAR covariance matrix is converted into the standard SAR intensity which puts the standard statistical models for SAR to be within the natural coverage of this generic models for POLSAR. All of these theoretical developments are then validated against real-life practical data in section V. Finally section VI concludes the paper by briefly describing how an existing SAR data processing technique can be adapted for POLSAR data.

II. Related Work in Literature

This section critically review the related work in published literature. Specifically, the first subsection reviews various scalar statistical models for different POLSAR observables. Its purpose is to show that none of the proposed models have led to statistically consistent discrimination

measures. The second sub-section strengthen this findings by reviewing many different discrimination measures that have been proposed for POLSAR data. It shows that almost all of them depends on the likelihood statistical test for complex Wishart distribution. Unfortunately, in the original proposed work [1] for the test, while an exact distribution is to be expected, only an asymptotic distribution was given.

A. Scalar Observables and Statistical Models for POLSAR Data

Different target decomposition theorems have identified many different scalar observables for the complex POLSAR data. In [2], the performance of different scalar POLSAR observables for classification purposes is evaluated. While many scalar observables for POLSAR were presented, their corresponding statistical models and classifiers were not available. Furthermore, at its conclusion, the paper indicated that: "it is impossible to identify the best representation" for that purpose. To be fair, these observables are identified to describe a decomposed portion of the complex POLSAR data, and thus they are not to be used individually for the purpose of single-handedly representing POLSAR data.

Given the joint distribution for POLSAR is known to be the multi-variate Complex Wishart distribution, it is possible to derive the scalar statistical models for some univariate POLSAR observables. This is is the foundation of another thread of studies in POLSAR. However, such derivations are no trivial tasks, and so far, only a handful of such statistical models have been proposed. In the field of POLSAR, the list includes:

1) cross-pol ratio $r_{HV/HH} = |S_{HV}|^2/|S_{HH}|^2$ [3],
2) co-pol ratio $r_{VV/HH} = |S_{VV}|^2/|S_{HH}|^2$ [3],
3) co-pol phase difference $\phi_{VV/HH} = arg(S_{VV}S^*_{HH})$ [3] [4],
4) magnitude $g = |avg(S_{pq}S^*_{rs})|$ [4],
5) normalized magnitude $\xi = \frac{|avg(S_{pq}S^*_{rs})|}{\sqrt{avg(|S_{pq}|^2)avg(|S_{rs}|^2)}}$ [4],
6) intensity ratio $w = avg(|S_{pq}|^2)/avg(|S_{rs}|^2)$ [4],
7) and the Stokes parameters $S_i, 0 \leq i \leq 3$ [5].

Furthermore, recently the statistical models for each element of the POLSAR covariance matrix $S_{pq}S^*_{rs}$ [6] as well as for the largest eigen-value of the covariance matrix λ_1 [7] have been studied. While these models undoubtedly help in understanding the SAR data, individually none of these

observables has been shown to statisfy the dual criteria of 1) resulting in statistically consistent discrimination measures and 2) being representative of the complex POLSAR data.

B. POLSAR Discrimination Measures

This sub-section reviews some relevant and published works relating to different measures of distance for POLSAR data. In particular, a few different matrix distances have been proposed and evaluated in recent review papers [8] [9] will be briefly reviewed.

The commonly used measure of distance for matrices are either the Euclidean or the Manhattan distance, which are defined in the following equations, respectively:

$$d(C_x, C_y) = \sum_{i,j} |\mathbb{R}(C_x - C_y)_{i,j}| + \sum_{i,j} |\mathbb{I}(C_x - C_y)_{i,j}| \tag{1}$$

$$d(C_x, C_y) = \sqrt{\sum_{i,j} |C_x - C_y|^2_{i,j}} \tag{2}$$

where $A_{i,j}$ denotes the (i,j) elements of the matrix A, $||$ denotes absolute values and $\mathbb{R}, \mathbb{I}$ denote the real and imaginary parts respectively. However, in the context of POLSAR covariance matrix, these dis-similarity measures are not widely used probably because of the multiplicative nature of the data.

In the field of POLSAR, the Wishart Distance is probably the most widely used as part of the well-known Wishart Classifier [10]. The distance is defined as [11]

$$d(C_x, C_y) = \ln |C_y| + tr(C_x C_y^{-1}) \tag{3}$$

As a measure of distance, its main disadvantage is that $d(C_y, C_y) = \ln |C_y| \neq 0$.

Recent works have suggested a number of other dissimilarity measures. These include the asymmetric and symmetric refined wishart distance [12],

$$d(C_x, C_y) = \frac{1}{2} tr(C_x^{-1} C_y + C_y^{-1} C_x) - d \tag{4}$$

$$d(C_x, C_y) = \ln |C_x| - \ln |C_y| + tr(C_x C_y^{-1}) - d \tag{5}$$

the Bartlett distance [9],

$$d(C_x, C_y) = 2 \ln |C_{x+y}| - \ln |C_x| - \ln |C_y| - 2d \ln 2 \tag{6}$$

the Bhattacharyya distance [13],

$$r(C_x, C_y) = \frac{|C_x|^{1/2}|C_y|^{1/2}}{|(C_x + C_y)/2|} \tag{7}$$

and the Wishart Statistical test distance [14]

$$d(C_x, C_y) = (L_x + L_y)\ln|C| - L_x \ln|C_x| - L_y \ln|C_y| \tag{8}$$

.

Closer investigation of these dis-similarity measures reveals that most of them are related to each other. The Bhattacharyya distance is easily shown to be related to the Barlett distance. At the same time the Barlett distance can be considered as the special case of the Wishart Statistical Test distance, where the two data set have the same number of look, i.e. $L_x = L_y$. The close relation among these is further supported by the fact that all of the papers proposing these measures referenced the statistical model developed in [1] as their foundation. In [1], to determine if the two scaled multi-look POLSAR covariance matrix Z_x and Z_y, which have L_x and L_y as the corresponding number of looks, come from the same underlying stochastic process, the likelihood ratio statistics for POLSAR covariance matrix is considered:

$$Q = \frac{(L_x + L_y)^{d\cdot(L_x+L_y)}}{L_x^{d\cdot L_x} L_y^{d\cdot L_y}} \frac{|Z_x|^{L_x}|Z_y|^{L_y}}{|Z_x + Z_y|^{(L_x+L_y)}}$$

Taking the log-transformation of the above statistics, and note that $C_{vx} = Z_x/L_x$, $C_{vy} = Z_y/L_y$ and $C_{vxy} = (Z_x + Z_y)/(L_x + L_y)$ it becomes

$$Q = \frac{|C_{vx}|^{L_x} \cdot |C_{vy}|^{L_y}}{|C_{vxy}|^{L_x+L_y}} \tag{9}$$

$$\ln Q = L_x \ln|C_{vx}| + L_y \ln|C_{vy}| - (L_x + L_y)\ln|C_{vxy}| \tag{10}$$

To detect changes, a test statistics is developed based on this measure of distance. This means a distribution is to be derived for the dissimilarity measure. However, originally in the proposed work [1], only an asymptotic distribution is derived.

III. The Scalar Statistical Models for POLSAR

In this section, several scalar statistical models for POLSAR are presented. After the first sub-section briefly introduce the basic foundations, concepts and notation of this paper the second sub-section presents the theoretical models together with conclusive evidence for two related points. The first point is that: POLSAR data is multiplicative and heteroskedastic in its original

domain. And the second conclusion being: log-transformation converts it into an additive and homoskedastic model. Consequently a few consistent measures of distance are presented in the final sub-section.

A. The Basics of POLSAR Statistical Analysis

In this paper, the POLSAR scattering vector is denoted as s. In the case of partial polarimetric SAR (single polarization in transmit and dual polarization in receipt), the vector is two-dimensional ($d = 2$) and is normally written as:

$$s_{part} = \begin{bmatrix} S_h \\ S_v \end{bmatrix} \tag{11}$$

In the case of full and monostatic POLSAR data, the vector is three-dimensional ($d = 3$) and is presented as:

$$s_{full} = \begin{bmatrix} S_{hh} \\ \sqrt{2}S_{hv} \\ S_{vv} \end{bmatrix} \tag{12}$$

Let $\Sigma = E[ss^{*T}]$ denote the population expected value of the POLSAR covariance matrix, where s^{*T} denotes the complex conjugate transpose of s. Assuming s is jointly circular complex Gaussian with the expected covariance matrix Σ, then the probably density function (PDF) of s can be written as:

$$pdf(s;\Sigma) = \frac{1}{\pi^d|\Sigma|}e^{-s^{*T}\Sigma^{-1}s} \tag{13}$$

where $||$ denotes the matrix determinant.

The sample POLSAR covariance matrix is formed as the mean of Hermitian outer product of independent single-look scattering vectors,

$$C_v = \langle ss^{*T} \rangle = \frac{1}{L}\sum_{i=1}^{L} s_i s_i^{*T} \tag{14}$$

where s_i denotes the single-look scattering vector, which equals s_{part} in the case of partial POLSAR and s_{full} in the case of full polarimetry, and L is the number of looks.

Complex Wishart distribution statistics, however, are normally written for the scaled covariance matrix $Z = LC_v$, whose PDF is given as:

$$pdf(Z;d,\Sigma,L) = \frac{|Z|^{L-d}}{|\Sigma^L|\Gamma_d(L)}e^{-tr(\Sigma^{-1}Z)} \tag{15}$$

with $\Gamma_d(L) = \pi^{d(d-1)/2} \prod_{i=0}^{d-1} \Gamma(L-i)$ and d is the dimensional number of the POLSAR covariance matrix.

The approach taken in this paper differs by applying the homoskedastic log transformation on a less-than-well-known result for the determinant of the covariance matrix. Goodman [15] proved that the ratio between the observable and expected values of the sample covariance matrix's determinants behave like a product of d chi-squared random variables with different degrees of freedom

$$\chi_L^d = (2L)^d \frac{|C_v|}{|\Sigma_v|} \sim \prod_{i=0}^{d-1} \chi^2(2L-2i) \tag{16}$$

Its log-transformed variable consequently behaves like a summation of d log-chi-squared random variables with the same degrees of freedom

$$\Lambda_L^d = ln\left[(2L)^d \frac{|C_v|}{|\Sigma_v|}\right] \sim \sum_{i=0}^{d-1} \Lambda^\chi(2L-2i) \tag{17}$$

with $\Lambda^\chi(k) \sim \ln\left[\chi^2(k)\right]$

B. Original Hetoroskedastic Domain and the Homoskedastic Log-Transformation

In this section the multiplicative nature of POLSAR data is first illustrated. Log-transformation is then used to convert the data into a more familiar additive model. Heteroskedasticity, which is defined as the dependence of variance upon the underlying signal, is shown to be the case for the original POLSAR data. In log-transformed domain, the case for a homoskedastic model, where sample variance is fixed and thus independent of the underlying signal, is demonstrated. To keep the section flowing, the mathematical derivation is only presented here in major sketches. For more detailed derivation, Appendix A should be referred to.

From Eqns. 16 and 17 we can deduce the following relationships:

$$|C_v| \sim |\Sigma_v| \cdot \frac{1}{(2L)^d} \cdot \prod_{i=0}^{d-1} \chi^2(2L-2i) \tag{18}$$

$$\ln|C_v| \sim \ln|\Sigma_v| - d \cdot \ln(2L) + \sum_{i=0}^{d-1} \Lambda(2L-2i) \tag{19}$$

In a given homogeneous POLSAR area, the parameters Σ_v, d and L can be considered as constant. Thus Eqn. 18 gives the theoretical explaination that: in the original POLSAR domain,

a multiplicative speckle noise pattern is present. At the same time, Eqn. 19 shows that the logarithmic transformation has converted this to the more familiar additive noise.

Since chi-squared random variables $X \sim \chi^2(k)$ follows a known PDF:

$$pdf(x;2L) = \frac{x^{L-1}e^{-x/2}}{2^L\Gamma(L)} \tag{20}$$

applying the variable change theorem, its log-transformed variable follows the PDF of:

$$pdf(x;2L=k) = \frac{e^{Lx-e^x/2}}{2^L\Gamma(L)} \tag{21}$$

As the PDFs become available, the characteristic functions (CF) of both the chi-squared and log-chi-squared random variables can be written as:

$$CF_\chi(t) = (1-2it)^L \tag{22}$$

$$CF_\Lambda(t) = 2^{it}\frac{\Gamma(L+it)}{\Gamma(L)} \tag{23}$$

Subsequently their means and variances can be computed from the given characteristic functions. They are:

$$avg\left[\chi(2L)\right] = 2L \tag{24}$$

$$var\left[\chi(2L)\right] = 4L \tag{25}$$

$$avg\left[\Lambda(2L)\right] = \psi^0(L) + \ln 2 \tag{26}$$

$$var\left[\Lambda(2L)\right] = \psi^1(L) \tag{27}$$

where $\psi^0()$ and $\psi^1()$ represent the digamma and trigamma functions respectively.

Since the average and variance of both chi-squared distribution and log-chi-squared distribution are constant, the product and summation of these random variables also has fixed summary statistics. Specifically:

$$avg\left[\prod_{i=0}^{d-1}\chi^2(2L-2i)\right] = 2^d\cdot\prod_{i=0}^{d-1}(L-i),$$

$$var\left[\prod_{i=0}^{d-1}\chi^2(2L-2i)\right] = \prod_{i=0}^{d-1}4(L-i)(L-i+1) - \prod_{i=0}^{d-1}4(L-i)^2,$$

$$avg\left[\sum_{i=0}^{d-1}\Lambda(2L-2i)\right] = d\cdot\ln 2 + \sum_{i=0}^{d-1}\psi^0(L-i),$$

$$var\left[\sum_{i=0}^{d-1}\Lambda(2L-2i)\right] = \sum_{i=0}^{d-1}\psi^1(L-i)$$

Combining these results with Eqns. 18 and 19, we have:

$$avg\left[|C_v|\right] = \frac{|\Sigma_v|}{L^d}\prod_{i=0}^{d-1}(L-i) \tag{28}$$

$$var\left[|C_v|\right] = \frac{|\Sigma_v|^2\left[\prod_{i=0}^{d-1}(L-i)(L-i+1) - \prod_{i=0}^{d-1}(L-i)^2\right]}{L^{2d}} \tag{29}$$

$$avg\left[\ln|C_v|\right] = \ln|\Sigma_v| - d\cdot\ln L + \sum_{i=0}^{d-1}\psi^0(L-i) \tag{30}$$

$$var\left[\ln|C_v|\right] = \sum_{i=0}^{d-1}\psi^1(L-i) \tag{31}$$

For a real world captured image, while the parameters d and L do not change for the whole image, the underlying Σ_v is expected to differ from one region to the next. Thus over an heterogeneous scene, the stochastic process for $|C_v|$ and $\ln|C_v|$ varies depending on the underlying signal Σ_v. In such context, Eqn. 29 implies that the variance of $|C_v|$ also differs depending on the underlying signal Σ_v, which indicates its heteroskedastic property. At the same time, in the log-transformed domain, Eqn. 31 reveals that the variance of $\ln|C_v|$ is invariant and independent of Σ_v manifesting its homoskedastic nature.

C. Consistent Measures of Distance for POLSAR

Similar to the way dispersion and contrast is defined in our previous work [16] [17], this section introduces the consistent sense of distance from a couple of different perspectives. Assuming, on the one hand, that the true value of the underlying signal Σ_v is known *a priori*, random variables, ratio ($\mathbb{R}$) and log-distance ($\mathbb{L}$), are observable according to their definitions:

$$\mathbb{R} = \frac{|C_v|}{|\Sigma_v|} \tag{32}$$

$$\mathbb{L} = \ln|C_v| - \ln|\Sigma_v| \tag{33}$$

On the other hand, under a more forgiving assumption where the POLSAR is known to have come from a homogeneous area, but the true value of the underlying signal Σ_v is *unknown*, the dispersion ($\mathbb{D}$) and contrast ($\mathbb{C}$) random variables are observable and they are defined as:

$$\mathbb{D} = \ln|C_v| - avg(\ln|C_v|) \tag{34}$$

$$\mathbb{C} = \ln(|C_{v1}|) - \ln(|C_{v2}|) \tag{35}$$

Using the results from Eqns. 18, 19 and 30 we have

$$\mathbb{R} \sim \frac{1}{(2L)^d} \cdot \prod_{i=0}^{d-1} \chi^2(2L-2i) \tag{36}$$

$$\mathbb{L} \sim \sum_{i=0}^{d-1} \Lambda(2L-2i) - d \cdot \ln(2L) \tag{37}$$

$$\mathbb{D} \sim \sum_{i=0}^{d-1} \Lambda(2L-2i) - d \cdot \ln 2 + k \tag{38}$$

$$\mathbb{C} \sim \sum_{i=0}^{d-1} \Delta(2L-2i) \tag{39}$$

with $\Delta(2L) \sim \Lambda(2L) - \Lambda(2L)$ and $k = \sum_{i=0}^{d-1} \psi^0(L-i)$

Also given the characteristic functions (CF) for the elementary components $\Lambda(2L)$ written in Eqn. 23, Appendix B derives the characteristic functions for the summative random variables as:

$$CF_{\Lambda_L^d}(t) = \frac{2^{idt}}{\Gamma(L)^d} \prod_{j=0}^{d-1} \Gamma(L-j+it) \tag{40}$$

$$CF_{\mathbb{L}}(t) = \frac{1}{L^{idt}\Gamma(L)^d} \prod_{j=0}^{d-1} \Gamma(L-j+it) \tag{41}$$

$$CF_{\mathbb{D}}(t) = \frac{e^{ikt}}{\Gamma(L)^d} \prod_{j=0}^{d-1} \Gamma(L-j+it) \tag{42}$$

$$CF_{\Delta(2L)} = \frac{\Gamma(2L)B(L-it, L+it)}{\Gamma(L)^2} \tag{43}$$

$$CF_{\mathbb{C}}(t) = \prod_{j=0}^{d-1} \frac{\Gamma(2L-2j)B(L-j-it, L-j+it)}{\Gamma(L-j)^2} \tag{44}$$

Since each elementary component follows fixed distributions (i.e. $\chi^2(2L), \Lambda(2L), ...$), it is natural that these variables also follow fixed distributions. Moreover, they are independent of the underlying signal Σ_v.

IV. SAR AS THE SPECIAL CASE OF POLARIMETRIC SAR

The previous section has introduced the theoretical model for 3-dimensional $d = 3$ full polarimetric and two dimensional $d = 2$ partial polarimetry cases. In this section, the model is shown to be also applicable for the 1-dimensional $d = 1$ case. Physically this means the multi-dimensional

POLSAR dataset is collapsed into one-dimensional conventional SAR data. Mathematically, the sample covariance matrix is reduced to the sample variance and the determinant equates the scalar value. On the other hand, it is well known that for SAR data, variance equals intensity. Thus the special case of our result is investigated carefully and is shown to be consistent with previous results for SAR intensity data. This can be thought of either as a cross-validation evidence for the proposed POLSAR models or alternatively as having SAR as the special case of POLSAR.

The results so far for our models can be summarized using the following equations:

$$\mathbb{R} = \frac{|C_v|}{|\Sigma_v|} \sim \frac{1}{(2L)^d} \prod_{i=0}^{d-1} \chi^2(2L-2i) \tag{45}$$

$$\mathbb{L} = \ln|C_v| - \ln|\Sigma_v| \sim \sum_{i=0}^{d-1} \Lambda(2L-2i) - d \cdot \ln 2L \tag{46}$$

$$\mathbb{D} = \ln|C_v| - avg(\ln|C_v|) \sim \sum_{i=0}^{d-1} \Lambda(2L-2i) - d \ln 2 + k \tag{47}$$

$$\mathbb{C} = \ln|C_{1v}| - \ln|C_{2v}| \sim \sum_{i=0}^{d-1} \Delta(2L-2i) \tag{48}$$

$$\mathbb{A} = avg(\mathbb{L}) = \sum_{i=0}^{d-1} \psi^0(L-i) - d \cdot \ln L \tag{49}$$

$$\mathbb{V} = var(\mathbb{L}) = \sum_{i=0}^{d-1} \psi^1(L-i) \tag{50}$$

$$\mathbb{E} = mse(\mathbb{L}) = \left[\sum_{i=0}^{d-1} \psi^0(L-i) - d \cdot \ln L\right]^2 + \sum_{i=0}^{d-1} \psi^1(L-i) \tag{51}$$

Upon setting $d = 1$ into the above equations, Appendix C shows that the reduced results are consistent with the following two cases. First is the the following results obtained from the our

previous works on single-look SAR [16] [17], i.e. $d = L = 1$,

$$
\begin{aligned}
I &\sim \bar{I} \cdot pdf\left[e^{-R}\right] \\
\log_2 I &\sim \log_2 \bar{I} + pdf\left[2^x e^{-2^x} \ln 2\right] \\
\mathbb{R} &= \frac{I}{\bar{I}} \sim pdf\left[e^{-x}\right] \\
\mathbb{L} &= \log_2 I - \log_2 \bar{I} \sim pdf\left[2^x e^{-2^x} \ln 2\right] \\
\mathbb{D} &= \log_2 I - avg(\log_2 I) \sim pdf\left[e^{-(2^x e^{-\gamma})} 2^x e^{-\gamma} \ln 2\right] \\
\mathbb{C} &= \log_2 I_1 - \log_2 I_2 \sim pdf\left[\frac{2^x}{(1+2^x)^2} \ln 2\right] \\
\mathbb{A} &= avg(\mathbb{L}) = -\gamma / \ln 2 \\
\mathbb{V} &= var(\mathbb{L}) = \frac{\pi^2}{6} \frac{1}{\ln^2 2} \\
\mathbb{E} &= mse(\mathbb{L}) = \frac{1}{\ln^2 2}(\gamma^2 + \pi^2/6) = 4.1161
\end{aligned}
$$

The second is the following well-known results for multi-look SAR, i.e. $d = 1, L > 1$:

$$
I \sim pdf\left[\frac{L^L x^{L-1} e^{-Lx/\bar{I}}}{\Gamma(L)\bar{I}^L}\right] \tag{52}
$$

$$
N = \ln I \sim pdf\left[\frac{L^L}{\Gamma(L)} e^{L(x-\bar{N}) - Le^{x-\bar{N}}}\right] \tag{53}
$$

Furthermore, the following derivations for multi-look SAR data show that it can be thought of either as extensions of the corresponding single-look SAR results or as simple cases of the

POLSAR results are also derived as:

$$\mathbb{R} = \frac{I}{\bar{I}} \sim pdf\left[\frac{L^L x^{L-1} e^{-Lx}}{\Gamma(L)}\right]$$

$$\mathbb{L} = \ln I - \ln \bar{I} \sim pdf\left[\frac{L^L e^{Lt - Le^t}}{\Gamma(L)}\right]$$

$$\mathbb{D} = \ln I - avg(\ln I) \sim pdf\left[\frac{e^{L[x-\psi^0(L)]-e^{[x-\psi^0(L)]}}}{\Gamma(L)}\right]$$

$$\mathbb{C} = \ln I_1 - \ln I_2 \sim pdf\left[\frac{e^x}{(1+e^x)^2}\right]$$

$$\mathbb{A} = avg(\mathbb{L}) = \psi^0(L) - \ln L$$

$$\mathbb{V} = var(\mathbb{L}) = \psi^1(L)$$

$$\mathbb{E} = mse(\mathbb{L}) = \left[\psi^0(L) - \ln L\right]^2 + \psi^1(L)$$

This newly derived models for multi-look SAR data can also be validated against real-life data. Fig. 1 presents the results of an experiment carried out for the stated purpose. In the experiment the intensity of a single-channel SAR data (HH) for a homogeneous area in the AIRSAR Flevoland dataset is extracted. The histograms for the log-distance and contrast is then plotted against the theoretical PDF given above. The plot is obtained with ENL set to the nominal number of 4, and good visual match is apparent in the final results.

V. Validating the proposed models against real-life data

This section validates the theoretical models developed above against real-life practical data. The first sub-section provides a naive validation, where the nominal ENL is used for the model. While the match appears to be reasonably good, it can be further improved. After the second sub-section discusses why the nominal look-number given by (POL)SAR processors may not be very accurate, the third sub-section proposes a new technique in estimating the Effective Number of Looks (ENL) using the consistent variance found in homoskedastic model. With the newly estimated ENL, the final sub-section shows that the match between the theoretical model and the practical data is indeed further improved.

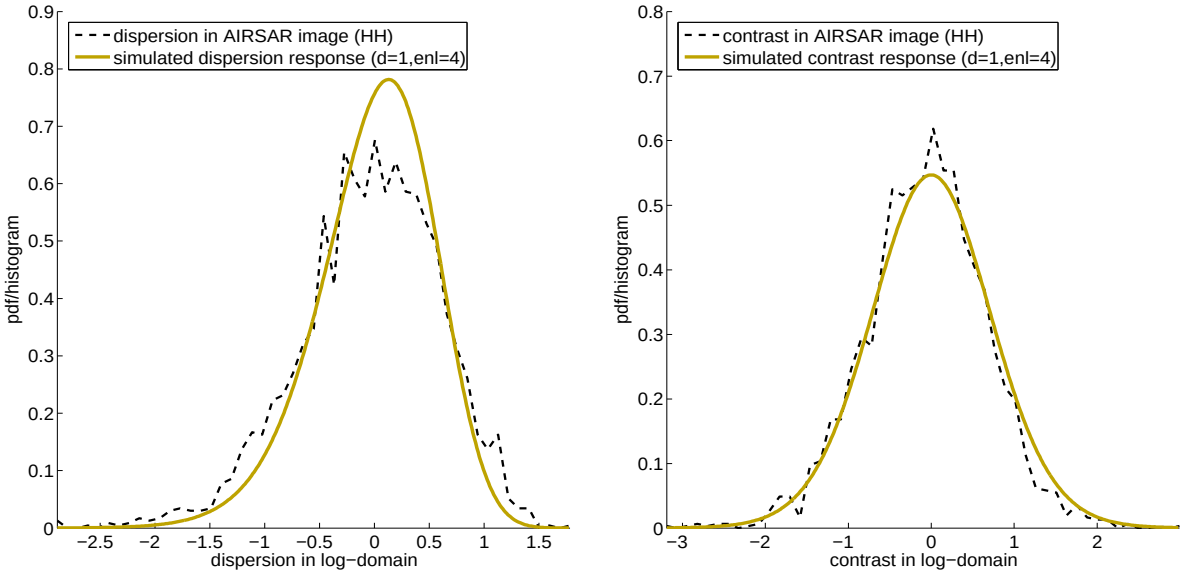

(a) multi-look SAR log-distance (b) multi-look SAR contrast

Fig. 1: Multi-Look SAR dispersion and contrast: modelled response matches very well with real-life captured data.

A. Using the nominal ENL to validate the theoretical models

This sub-section describes an experiment to validate the models presented earlier against real-life captured data, which can be performed in a rather straightforward manner. The stochastic models derived in the previous sections can be graphically visualized as histogram plots of the simulated data. At the same time, the form of the real-life practical data is also observable via the histogram plots of the data samples extracted from an homogeneous area. Therefore, the theoretical models can be validated if for the same parameters the two plots match each other reasonably well.

For this purpose, a homogeneous area was chosen from the AIRSAR Flevoland POLSAR data as experimental data samples. Then theoretical models are used to explain the data. All the newly proposed models is to be validated. They include: the determinant and its log-transformed models, together with the dissimilarity measures namely: the determinant ratio, log-distance, dispersion and the contrast measures of distance.

These models are closely related. For the same parameter set, the determinant and determinant

ratio are simply scaled versions of each other. Meanwhile, the log-determinant, log-distance and dispersion are also just shifted versions of each other. Hence one could expect that once a model is validated, the other models in the set will follow suit, assuming that all the parameters of the image are known.Nevertheless, all the models will be separately evaluated in this experiment to describe an interesting phenomenon.

Among all these models, the least-assumed stochastic process for dispersion and contrast measures of distance are validated first. For each pixel in the region, the determinant of the covariance matrix is computed and the log-transformation is applied. Then the average of log-determinant of the POLSAR covariance matrix, i.e. $avg(ln|C_v|)$, is measured for dispersion. Subsequently the observable samples of dispersion and contrast are computed according to Eqns. 34 and 35 in order to plot their histograms.

At the same time, theoretical simulations according to Eqns. 38 and 39 are carried out. Here the nominal look-number is employed $L = 4$ for this experiment, while the dimensional number is set to either 3 or 2 depending on whether a full or partial polarimetric SAR dataset is being investigated. The plots are presented in Fig. 2 showing an evidentlt and visually match between the model and real data, effectively validating the theoretical models for dispersion and contrast.

Apart from dispersion and contrast, the other four models to be investigated require an estimation of the "true" underlying signal $|\Sigma_v|$. There are two ways to estimate this quantity over an homogeneous area. The traditional way is to simply set the true signal equal to the average of the POLSAR covariance matrix in its original domain, i.e. $\Sigma_v = avg(C_v)$. Another approach is to estimate the true signal from the average of the log-determinant of the POLSAR covariance matrix (i.e. $avg[ln|C_v|]$) using Eqn. 30. Both approaches will be presented in this section. As the log-determinant average has already been computed earlier, the second approach is hence used first for the validation of determinant-ratio and log-distance.

Fig. 3 plots the determinant-ratio and log-distance models against real-life data. In this experiment, the theoretical models are simulated using Eqns 36 and 37, while the observable samples are computed using Eqns 32 and 33 with the true signal estimated from the log-determinant average, i.e. $avg(\ln|C_v|)$. A reasonable match is again observed which validates the models for log-distance and determinant ratio.

Since the models for the determinant and log-determinant are just scaled or shifted version of the models for determinant-ratio and log-distance, similar validation results are to be expected.

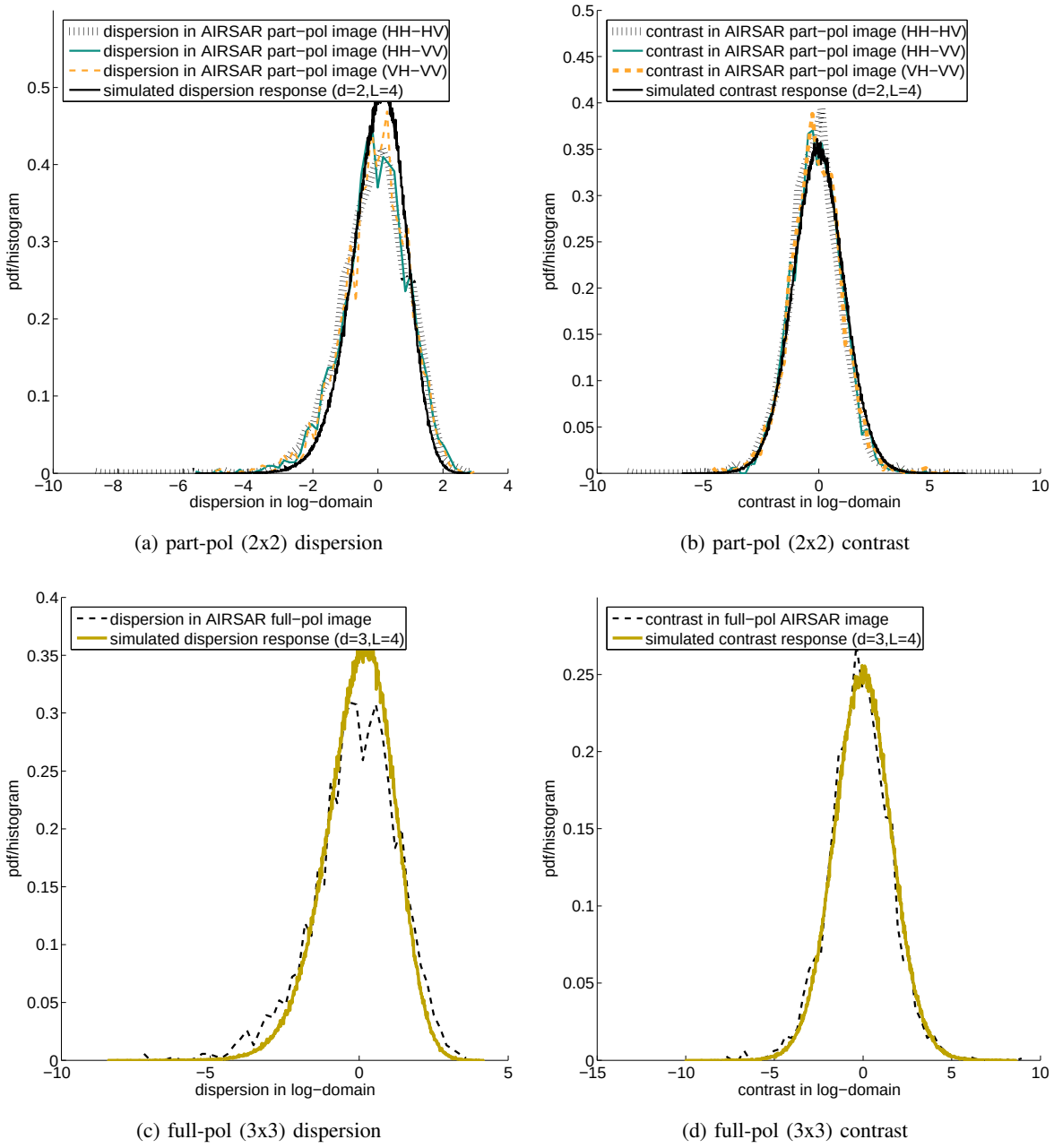

(a) part-pol (2x2) dispersion

(b) part-pol (2x2) contrast

(c) full-pol (3x3) dispersion

(d) full-pol (3x3) contrast

Fig. 2: Validating the dispersion and contrast models against both partial and full polarimetric AIRSAR Flevoland data.

However, a more subtle observation phenomena occurs during the validation process for the determinant and its log-transformed model, where the theoretical response is taken from the simulated stochastic process described by Eqns. 18 and 19. The phenomena happens when the

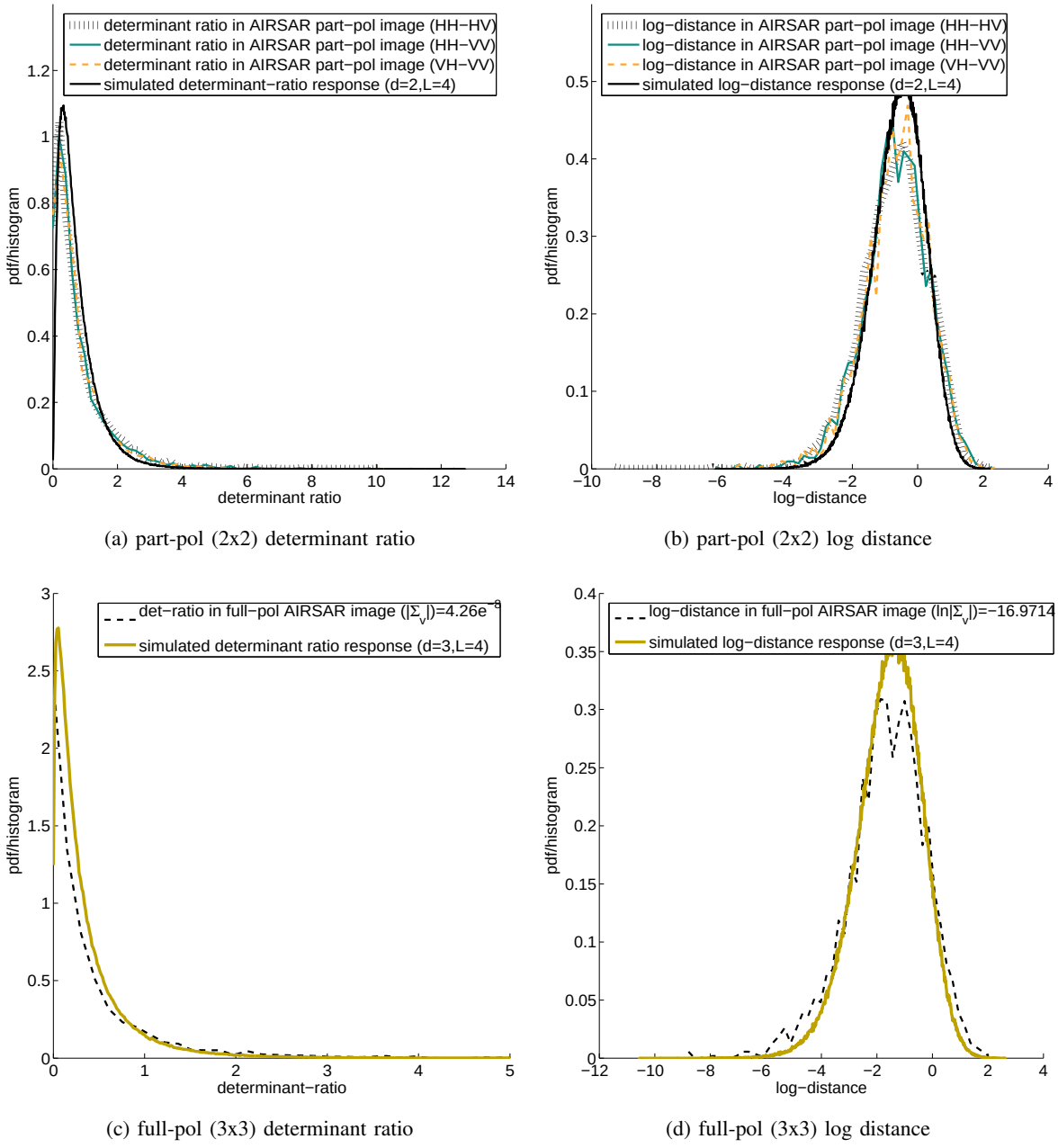

(a) part-pol (2x2) determinant ratio

(b) part-pol (2x2) log distance

(c) full-pol (3x3) determinant ratio

(d) full-pol (3x3) log distance

Fig. 3: Validating determinant-ratio and log-distance models with $|\Sigma_v|$ is computed using $avg(\ln|C_v|)$

true signal is estimated by the first approach i.e. equal to the average of the sample covariance matrix in its original domain (which evidently results in a different estimation for the true signal when compared with the method applied earlier). Subsequently the validation plots, which are

presented in Fig 4, exhibit some small translation and scaling discrepancies.

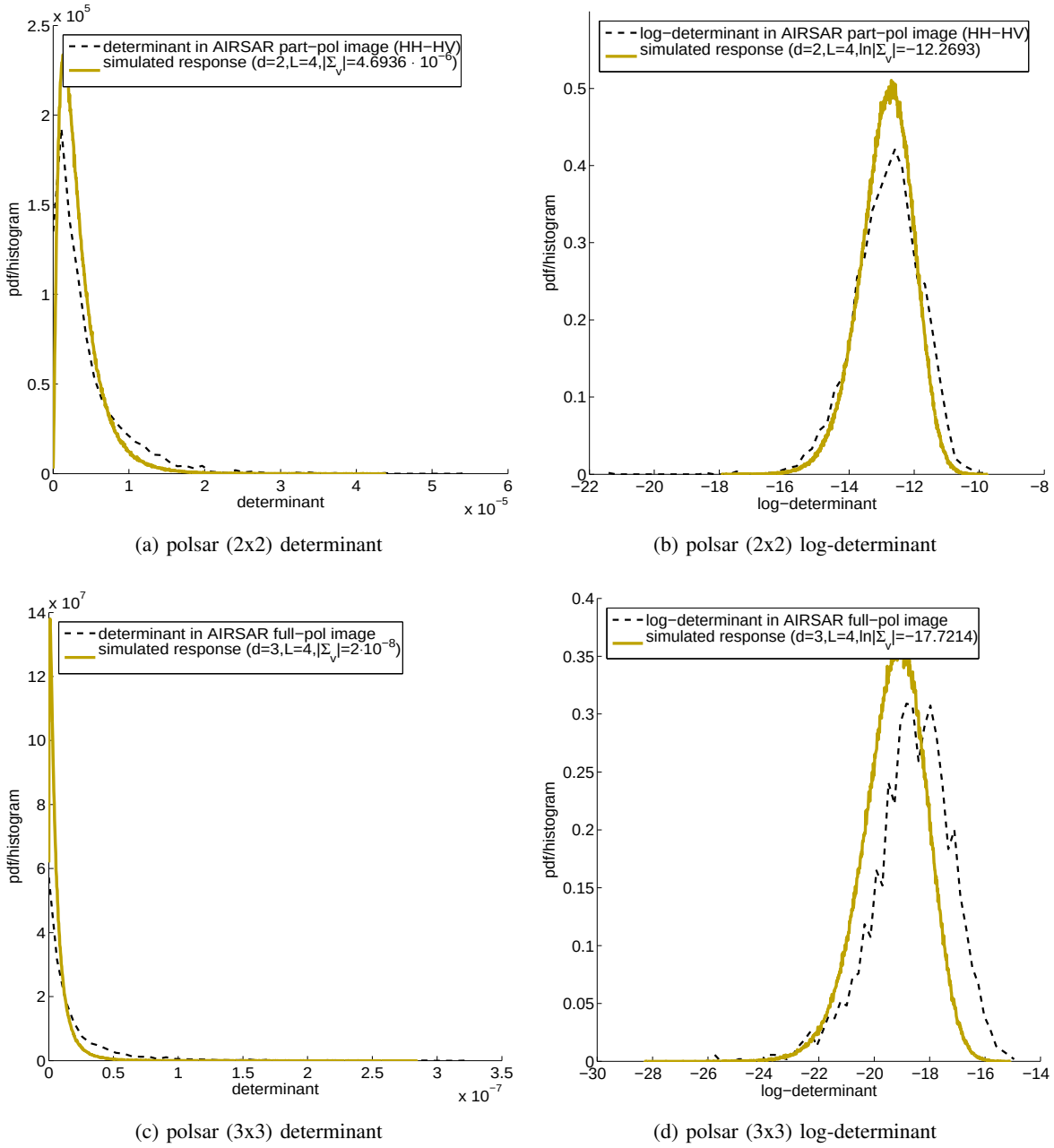

(a) polsar (2x2) determinant

(b) polsar (2x2) log-determinant

(c) polsar (3x3) determinant

(d) polsar (3x3) log-determinant

Fig. 4: Validating determinant and log-determinant models with $\Sigma_v = avg(C_v)$

In short the least-assumed dispersion and contrast measures of distance are shown to match reasonably well with the practical data. The same can be stated for the other four models, namely: determinant, log-determinant, determinant ratio and log-distance, if the underlying parameters

can be estimated reasonably well for the given image. However as described above a single "true signal" $|\Sigma_v|$ can have two different estimated values, depending on which estimation method was being used. The discrepancy suggests that at least one parameter for the models was inaccurately estimated. In fact, the next sub-section specifically indicates that the nominal look-number given by the (POL)SAR processor may not accurately reflect the true nature of the captured data.

B. The difference between the theoretical models and the practical data

Even though the assumptions made in developing this theory have intentionally been kept minimal, like all other similar models, the proposed model in this paper is built upon certain presumptions. Practical conditions however may not always satisfy these prerequisites. In this section, a common and observable gap between the conditions found in practical real-life data and the theoretical assumptions is discussed. And it is shown that: the theoretical model proposed can apply to the practical data, even when this "imperfection" is taken into account.

The assumption of statistical independence between samples (which applies to both SAR and POLSAR data) is reasonable given that the transmission and receipt of analogue signals is done independently for each radar pulse, i.e. for each resolution cell. Thus, theoretically speaking, adjacent pixels in an image can be assumed to be statistically independent. However, the actual imaging mechanism in a real-life (POL)SAR processor is that of a digital nature, where the analogue signal is to be converted into a digital data-set. Specifically, the analogue SAR signal, which is characterised by the pulse bandwidth measurement, is fed into an analogue-to-digital (ADC) sampling and conversion process which is characterised by its sampling rate. Theoretically it may be possible to define a sampling rate ensuring that each digital pixel corresponds exactly to an separate analogue physical cell. Practically however, to ensure "perfect reconstruction", the sampling rate is normally set at a slightly higher value than the Nyquist rate, resulting in a higher number of samples or pixels than the number of physical cells available in the scene.

Stated differently, in practice, each physical radar cell may be spread over more than a single pixel. This results in 1) a higher correlation between neighbouring pixels that may be related within a single physical cell resolution, and 2) reduced effective number of look, for example within a window of 3×3 pixels of a single-look image, it actually contains less than 9 physical analogue cells. The former phenomena is partially explained in [18] for SAR, while the later is experimental observed for POLSAR data in [4] and [19]. The oversampling practice is also

documented by the producers of SAR processors. For AIRSAR, the sampling rate and pulse bandwidth combinations are either 90/40MHz or 45/20MHz [20]. While for RadarSat2, the pixel resolution and range - azimuth resolution combination for SLC fine-quad mode is advertised as $(4.7 \cdot 5.1)m^2/(5.2 \cdot 7.7)m^2$ [21]

The proposed model can handle this imperfection that is found in practical data. The trick is that instead of using the nominal Number of Looks given by the SAR processor, an ENL estimation procedure is first undertaken, and subsequently the obtained ENL is then used. The next sub-section details a simple ENL estimation technique for POLSAR data. While the final sub-section demonstrates how the practical imperfection can be handled in a RADARSAT2 dataset. It also illustrates how the match shown in the first sub-section for the AIRSAR Flevoland dataset can be improved using ENL estimation.

C. ENL Estimation

The common approach in ENL estimation is to investigate the summary statistics of a known homogeneous area in the given data before making inferences about the inherent ENL. The summary statistics for $|C_v|$ and $\ln |C_v|$ have been derived in Section III-B, where Eqn. 30 indicates that there is a relationship among $|avg(C_v)|, avg(\ln |C_v|), d, L$. Recall that in carrying out the validation process using AIRSAR Flevoland data with nominal value $L = 4$, the relationship was shown to be broken. The reason is believed to be in the use of inexact value for L. In a given POLSAR datasat, since all values of $|avg(C_v)|, avg(\ln |C_v|), d$ are known, it is possible to estimate the "effective" number of look, by finding an L that ensures the above relationship is valid.

In fact, this approach was taken in [19], where an equation of exactly the same form as Eqn. 30 was used to estimate the ENL. Unfortunately, the only known way to solve the equation for the unknown L requires the use of an "iterative numerical method". Instead of relying on the equations for statistical mean to find ENL, we propose an approach that makes used of variance statistics in the homoskedastic log-domain to find ENL. Specifically, Eqn. 31 can be rewritten as:

$$var\left[ln|C_v|\right] = f(L) = \sum_{i=0}^{d-1} \psi^1(L-i) \tag{54}$$

where $\psi^1()$ again denotes the tri-gamma function.

Thus theoretically, given some measurable value for $var\left[ln|C_v|\right]$, one could solve the above equation for the unknown L, which would also require some iterative computations. Practically however, the shape of the right-hand-side can be pre-computed and for each computed value of $var\left[ln|C_v|\right]$, a corresponding value for L can be found by referencing the variance value on the pre-computed graph or by using the following equation:

$$\hat{L} = d\left(\frac{1}{var(\ln|C_v|)} + 0.5\right) \tag{55}$$

Fig. 5 shows the shapes of the function defined in Eqn. 54 for SAR and partial-POLSAR data $f_{d=1}(L)$ and $f_{d=2}(L)$ as well as illustrating the simplified approximation formula (Eqn. 55).

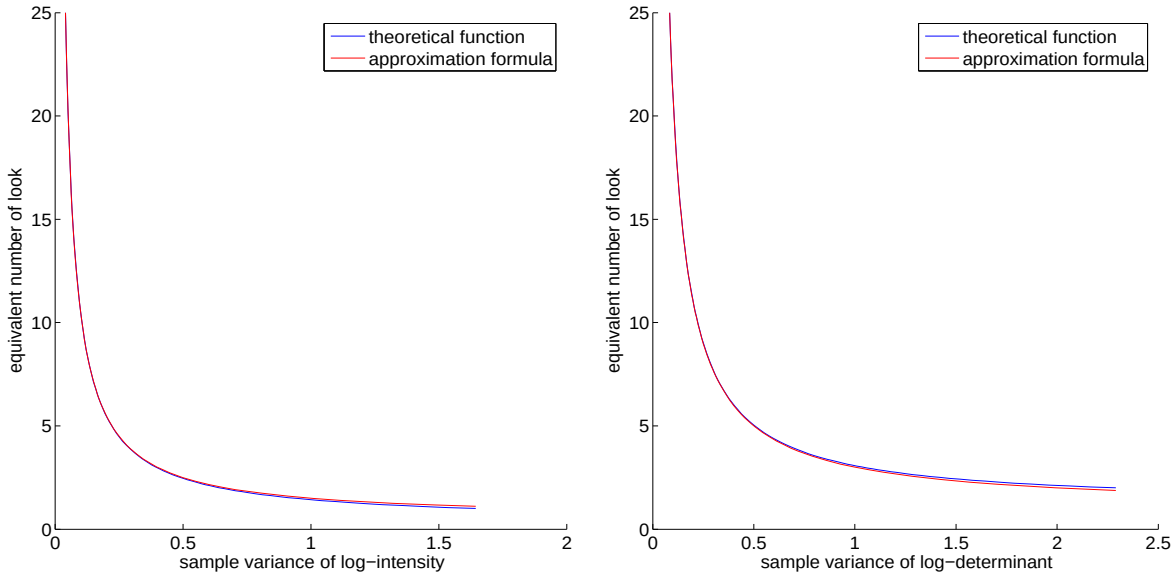

(a) ENL and variance log-intensity relations for SAR data (b) ENL and var(log-det) relations for partial POLSAR data

Fig. 5: The relations between ENL and sample variance of log-determinant/log-intensity

D. Using estimated ENL to better explain practical data

For this experiment an example single-look complex fine-quad RADARSAT2 dataset is used. Nine-look processing is applied before the dispersion histogram in the log-transformed domain is computed for a known homogeneous area. The histograms for both one-dimensional SAR and two-dimensional partial POLSAR data are plotted in Fig. 6 against the theoretical models for the nominal ENL value of 9. The match, however, is evidently not very close.

A better match can be achieved by first estimating ENL from the observable variance of the log-determinant, and the theoretical model is then simulated for the estimated ENL. Then the new sample histogram is plotted in the same figure, showing a much better consistency. This procedure can always be carried out for a given dataset, as long as a homogeneous area can be defined and extracted.

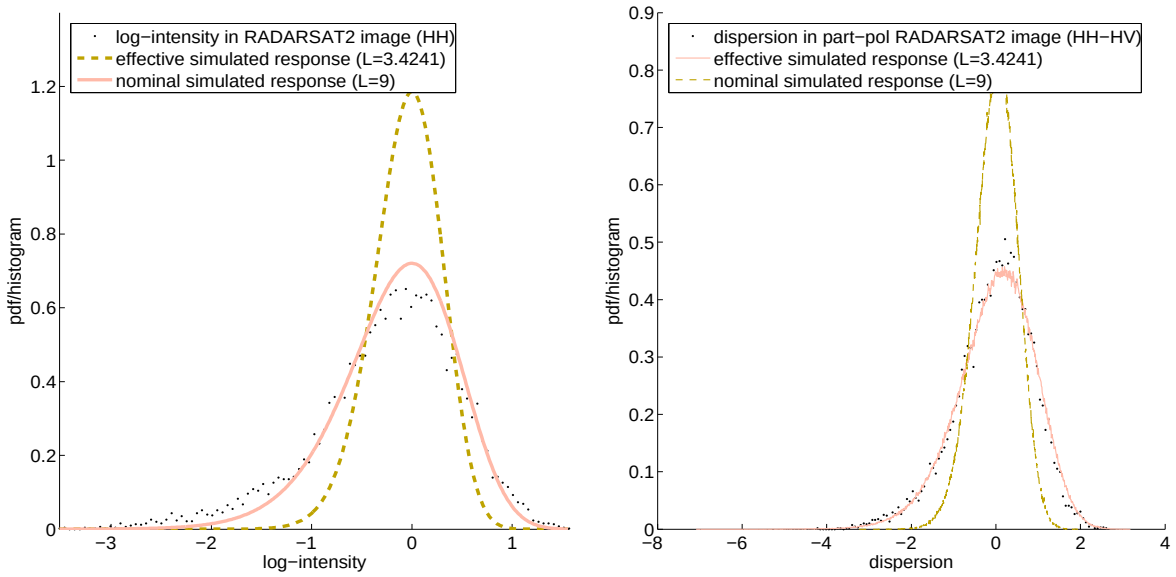

(a) Handling over-sampling practice in Radarsat2 one-dimensional SAR data (HH)

(b) Handling over-sampling practice in Radarsat2 partial POLSAR data (HH-HV)

Fig. 6: 9-look processed Radarsat2 data do not exactly exhibit 9-look data characteristics. Homoskedastic model in log-transformed domain can successfully estimate the effective ENL and then explain the data reasonably well.

Fig. 7 shows that the over-sampling issue is also present in the AIRSAR Flevoland dataset, even though it is to a much lesser-extent. Still, the "corrected" ENL offers an evidently better match between the model and real-life data.

VI. Discussion and Conclusion

A. Discussion

Let us begin the discussion by noting a few theoretical properties of the proposed statistical model. First, the use of covariance matrix log-determinant may be related to the standard eigen-

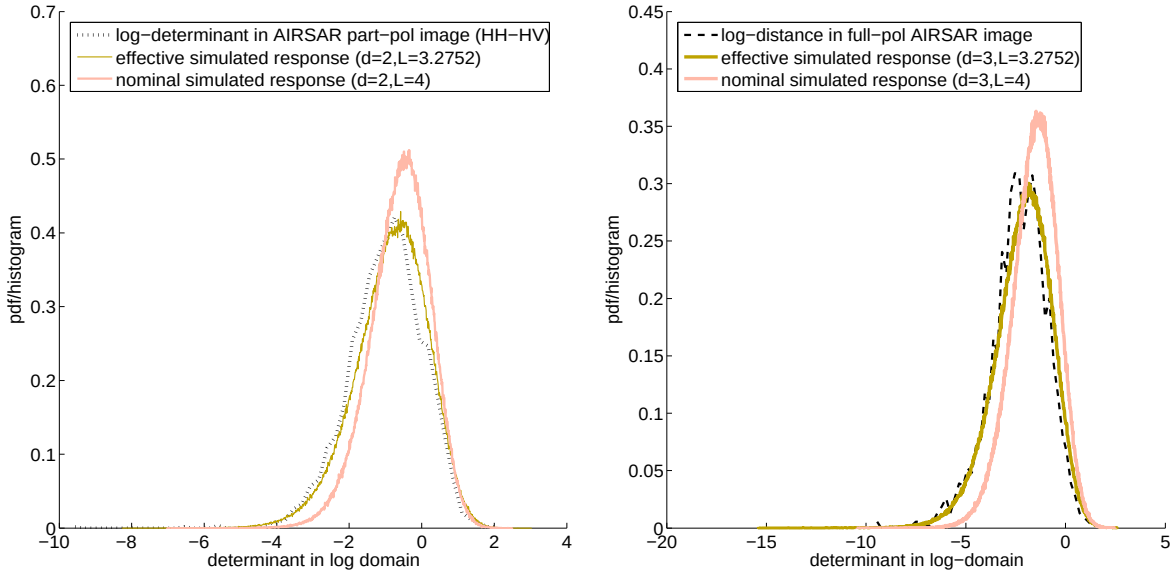

(a) Handling over-sampling practice in AIRSAR part-pol dataset

(b) Handling over-sampling practice in AIRSAR full-pol dataset

Fig. 7: AIRSAR Flevoland also exhibits phenomena of over-sampling practice, through at a lesser extend than the RADARSAT 2 data.

decomposition method of the POLSAR covariance matrices. In fact, the log-determinant can also be computed as the sum of log-eigenvalues. Specifically $\ln|M| = \sum \ln \lambda_M$ where λ_M denotes all the eigenvalues of M. Thus similar to other eigenvalue based approach (e.g. entropy/anisotropy, ...), the models presented here are invariant to polarization basis transformations.

Second, the model is developed for the POLSAR covariance matrix. However, since the POLSAR coherent matrix is related with the covariance matrix via an unitary transformation, which preserves the determinant, the model should also be applicable on the coherency matrix.

The model is far from complete. It calls for the reduction of the multi-dimensional POLSAR data into a scalar value. While this is probably desirable for a wide range of application where a one-dimensional number is required to represent the complex multi-dimensional data, such a reduction is unlikely to be lossless. Thus to better understand POLSAR data the use of this technique can be complemented with some high-dimensional POLSAR target-decomposition techniques (e.g. the Freeman Durden decomposition [22] or the entropy/anisotropy decomposition [23] ...).

However the proposed model is promising. Eventhough initially developed for partial and monostatic POLSAR data, they were then shown to be also applicable to traditional SAR data. Since the models assumptions are quite minimal, they may also be found to apply to bi-static and interferometric data, although that would require significant further investigations.

The theoretical models may also provide an alternative derivation for the widely used likelihood test statistics in POLSAR. In view of the models given in Eqns 18 & 19, the likelihood test statistics exposed in [1] and rewritten in Eqns 9 & 10 can be simulated as:

$$\ln Q \sim k + L_x \Lambda^d_{L_x} + L_y \Lambda^d_{L_y} - (L_x + L_y)\Lambda^d_{(L_x+L_y)}$$

$$Q \sim e^k \frac{(\chi^d_{L_x})^{L_x} \cdot (\chi^d_{L_y})^{L_y}}{(\chi^d_{L_x+L_y})^{L_x+L_y}}$$

where $k = d\left[(L_x + L_y)\ln(L_x + L_y) - L_x \ln L_x - L_y \ln L_y\right]$.

Similar to the way that other measures of distance can be used to derive POLSAR classifiers [10], change detectors [1], edge detectors [24] or other clustering and speckle filtering techniques [16] [25], new detection, classification, clustering or speckle filtering algorithms can be derived using the models presented in this paper. Moreover many of the existing techniques in SAR may be adaptable for POLSAR data. Here a quick example is provided.

In evaluating SAR speckle filters, the intensity ratio is widely used. Specifically, in its original multiplicative domain, the ratio of the filtered output and the noisy input image represents the noise being removed. Assuming a perfect filtering condition, the ratio image should contain only of the random noise. Thus a commonly used visual evaluation is just to plot the ratio image and see if any image feature has also been removed.

We will be showing that this technique is easily applicable in the problem of evaluating POLSAR speckle filters. Such an adaptation maps the SAR intensity ratio to the POLSAR determinant-ratio. In fact better results can be achived. In [26], it has been shown that the multiplicative ratio is not very well suited for digital image presentation, which is linear and additive in nature. Thus in this experiment, logarithmic transformation is applied to convert the multiplicative determinant-ratio to become the linear subtractive contrast.

To illustrate the above analysis, an experiment is carried out to evaluate the performance of 3×3 and5×5 boxcar POLSAR filters on the AIRSAR Flevoland partial polarimetric data (HH-HV). A square 700×700 pixel patch is extracted from the AIRSAR dataset, and the two POLSAR speckle filters applied to the patch. Then the log-determinant images of the filtered

outputs are displayed in Fig. 8. At the same time, the residual is computed for both filters, and the images are also displayed in the same figure.

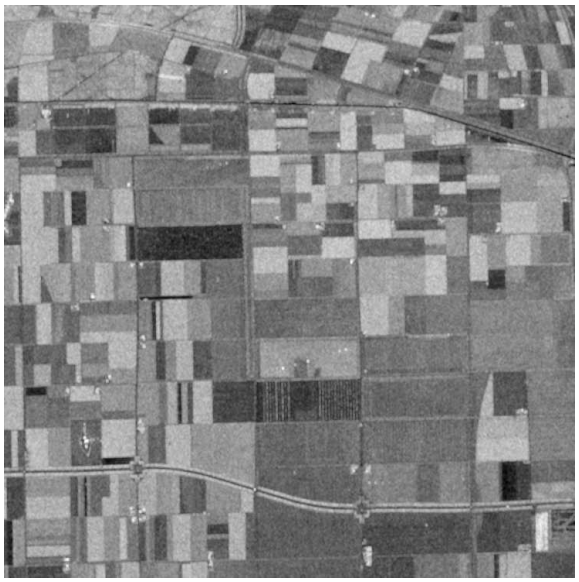

(a) Log-determinant Image of boxcar 3×3 speckle filter

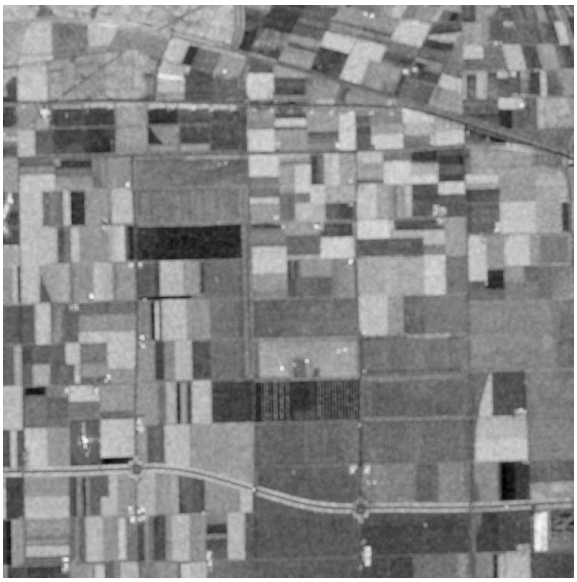

(b) Log-determinant Image of boxcar 5×5 speckle filter

(c) Image of Log-determinant Residual for 3×3 filter

(d) Image of Log-determinant Residual for 5×5 filter

Fig. 8: Visually Evaluating POLSAR Boxcar 3×3 vs. 5×5 Speckle Filters on AIRSAR Flevoland part-pol data (HH-HV) with expected MSE=1.0312 at ENL=4.

Fig. 8 shows that not only does the log-determinant image offer a nice visualization of the

scene, but also the distortion impact of the filter can also be made visible by the residual image. In visual evaluation, while it is quite hard to observe the worsening blurring-effects of the boxcar 5×5 speckle filter as compared to the 3×3 filter in the additive log-determinant image of the filtered output, such a conclusion can be made relatively easier by visualising the residual image.

There are many similar SAR data processing technique that may be adaptable to POLSAR. For example in the very same context of evaluating speckle filters, the mean and variance of the ratio image are also routinely used to provide quantitative evaluation. Evidently these techniques can also be adapted to evaluate POLSAR speckle filters, without much difficulties in foresight. In fact, we believe a list of such techniques would take pages. Here due to space restriction, only a simple example is described to highlight the beneficial implications of the proposed models.

B. Conclusion

In conclusion, a couple of scalar statistical models for the determinant of the POLSAR covariance matrix, which result in several consistent discrimination measures for POLSAR, are proposed and validated in this paper. The theoretical model is shown to be comprehensive in that: not only it can provide alternative and sometimes simpler explanations to a range of theoretical concepts such as POLSAR test statistics or ENL estimation, it also can be considered as the multi-dimensional extension of the traditionally used models for one-dimensional SAR data. Compared to other scalar statistical models for POLSAR, the proposed models are highly representative of the multi-dimensional POLSAR data.

The statistical model proposed in this paper is based on the determinant of the POLSAR covariance matrix which, when converted into one-dimensional data, is gracefully transformed into traditional SAR intensity. Consequently, the derived dissimilarity measures may be employed in a wide range of applications where a scalar number is required to represent the complex multi-dimensional POLSAR data. The models may also form a bridge, allowing the adaptation of many existing SAR data processing technique for POLSAR data, a quick example of this is briefly described in this paper.

APPENDIX A
HOMOSKEDASTIC MODEL FOR THE LOG-DETERMINANT

A. Log-Chi-Square Distribution and its Derivatives

This section provides the mathematical derivations for the log-transformed version of chi-squared random variables.

Chi-squared random variables $\chi \sim \chi^2(k)$ follows the pdf:

$$pdf(\chi;\, k) = \frac{\chi^{(k/2)-1} e^{-\chi/2}}{2^{k/2}\Gamma\left(\frac{k}{2}\right)} \tag{A.1}$$

Setting L=k/2 into Eqn. A.1

$$pdf(\chi) = \frac{\chi^{L-1} e^{-\chi/2}}{2^{L}\Gamma(L)} \tag{A.2}$$

Applying the variable change theorem, which states that: if $y = \phi(x)$ with $\phi(c) = a$ and $\phi(d) = b$, then:

$$\int_a^b f(y)\, dy = \int_c^d f[\phi(x)] \frac{d\phi}{dx} dx \tag{A.3}$$

into the log-transformation, which changes the random variables $\Lambda = ln(\chi)$, we have:

$$\begin{aligned} d\chi &= e^{\Lambda} d\Lambda \\ \frac{\chi^{L-1} e^{-\chi/2}}{2^{L}\Gamma(L)} d\chi &= \frac{(e^{\Lambda})^{L-1} e^{-e^{\Lambda}/2}}{2^{L}\Gamma(L)} e^{\Lambda} d\Lambda \end{aligned}$$

In other words, we have:

$$pdf(\Lambda; L) = \frac{e^{L\Lambda - e^{\Lambda}/2}}{2^{L}\Gamma(L)} \tag{A.4}$$

From the PDF given in Eqn. A.4, a characteristic function can be computed. By definition, the characteristic function (CF) $\varphi_X(t)$ for a random variable X is computed as:

$$\begin{aligned} \varphi_X(t) = \mathrm{E}\left[e^{itX}\right] &= \int_{-\infty}^{\infty} e^{itx}\, dF_X(x) \\ &= \int_{-\infty}^{\infty} e^{itx} f_X(x)\, dx \end{aligned}$$

with $\varphi_x(t)$ is the characteristic function, $F_X(x)$ is the CDF function of X and $f_X(x)$ is the PDF function of X. Thus the characteristic function for the log-chi-squared distribution is defined as:

$$\varphi_{\Lambda}(t) = \int_0^{\infty} e^{itx} \frac{e^{Lx - e^{x}/2}}{2^{L}\Gamma(L)}\, dx \tag{A.5}$$

The Gamma function is defined over the complex domain as: $\Gamma(z) = \int_0^\infty e^{-x}x^{z-1}dx$. Thus $\Gamma(L+it) = \int_0^\infty e^{-x}x^{L+it-1}dx$. Set $x = e^z/2$ then $dx = e^z/2dz$, we have $\Gamma(L+it) = \int_0^\infty e^{itz}\frac{e^{Lz-e^z/2}}{2^{L+it}}dz$

That is:

$$\varphi_\Lambda(t) = 2^{it}\frac{\Gamma(L+it)}{\Gamma(L)} \tag{A.6}$$

Consequently, the first and second derivative of the log-chi-squared distribution can be computed. The first derivative is given as:

$$\frac{\partial\varphi_\Lambda(t)}{\partial t} = \frac{i2^{it}\Gamma(L+it)}{\Gamma(L)}\left[\ln 2 + \psi^0(L+it)\right] \tag{A.7}$$

due to

$$\begin{aligned}
\frac{\partial\Gamma(x)}{\partial x} &= \Gamma(x)\psi^0(x),\\
\frac{\partial\Gamma(L+it)}{\partial t} &= i\Gamma(L+it)\psi^0(L+it),\\
\frac{\partial 2^{it}}{\partial t} &= i2^{it}\ln(2),\\
\partial(u\cdot v)/\partial t &= u\cdot\partial v/\partial t + v\cdot\partial u/\partial t,
\end{aligned}$$

where $\psi^0()$ denotes the di-gamma function.

Meanwhile, the second derivative can be written as:

$$\frac{\partial^2\varphi_\Lambda(t)}{\partial t^2} = \frac{i^2 2^{it}\Gamma(L+it)}{\Gamma(L)}\left(\left[\ln 2 + \psi^0(L+it)\right]^2 + \psi^1(L+it)\right) \tag{A.8}$$

due to:

$$\begin{aligned}
\frac{d2^{it}\Gamma(L+it)}{dt} &= i2^{it}\Gamma(L+it)\left[\ln 2 + \psi^0(L+it)\right],\\
\frac{d\psi^0(t)}{dt} &= \psi^1(t),\\
\frac{d\psi^0(L+it)}{dt} &= i\psi^1(L+it),\\
\partial(u\cdot v)/\partial t &= u\cdot\partial v/\partial t + v\cdot\partial u/\partial t,
\end{aligned}$$

with $\psi^1()$ denotes the tri-gamma function.

The n^{th} moments of random variable X can be computed from the derivatives of its characteristic function as:

$$\mathrm{E}\left(\Lambda^n\right) = i^{-n}\,\varphi_\Lambda^{(n)}(0) = i^{-n}\,\left[\frac{d^n}{dt^n}\varphi_\Lambda(t)\right]_{t=0} \tag{A.9}$$

Thus

$$\begin{aligned} \mathrm{E}\left(\Lambda\right) &= i^{-1}\left[\frac{d\varphi_{\Lambda}(t)}{dt}\right]_{t=0} \\ &= i^{-1}\left[\frac{i2^{it}\Gamma(L+it)}{\Gamma(L)}\left[\ln 2+\psi^{0}(L+it)\right]\right]_{t=0} \end{aligned}$$

That gives the result:

$$avg(\Lambda) = \psi^{0}(L) + ln(2) \tag{A.10}$$

Similarly, for the second moment,

$$\begin{aligned} \mathrm{E}\left(\Lambda^{2}\right) &= i^{-2}\left[\frac{d^{2}\varphi_{\Lambda}(t)}{dt^{2}}\right]_{t=0} \\ &= \left[\frac{2^{it}\Gamma(L+it)}{\Gamma(L)}\left(\left[\ln 2+\psi^{0}(L+it)\right]^{2}+\psi^{1}(L+it)\right)\right]_{t=0} \end{aligned}$$

That is equivalent to saying that

$$E(\Lambda^{2}) = \left[\psi^{0}(L)+\ln(2)\right]^{2}+\psi^{1}(L) \tag{A.11}$$

Thus we can state that

$$var(\Lambda) = E(\Lambda^{2}) - E^{2}(\Lambda) = \psi^{1}(L) \tag{A.12}$$

B. Averages and Variances of POLSAR Covariance Matrix Determinant and Log-Determinant

In this section, the expected value and variance value of these mixture of random variables are derived

$$\chi_{L}^{d} \sim \prod_{i=0}^{d-1}\chi(2L-2i) \tag{A.13}$$

$$\Lambda_{L}^{d} \sim \sum_{i=0}^{d-1}\Lambda(2L-2i) \tag{A.14}$$

given the averages and variances of individual components.

$$avg\left[\chi(2L)\right] = 2L \tag{A.15}$$

$$var\left[\chi(2L)\right] = 4L \tag{A.16}$$

$$avg\left[\Lambda(2L)\right] = \psi^{0}(L)+\ln 2 \tag{A.17}$$

$$var\left[\Lambda(2L)\right] = \psi^{1}(L) \tag{A.18}$$

Making use of the mutual independence property of each component X_i, the variance and expectation of the summation and product of random variables can be written as:

$$\begin{aligned} avg\left(\sum_{i=1}^{n} X_i\right) &= \sum_{i=1}^{n} avg(X_i), \\ var\left(\sum_{i=1}^{n} X_i\right) &= \sum_{i=1}^{n} var(X_i), \\ avg\left(\prod_{i=1}^{n} X_i\right) &= \prod_{i=1}^{n} avg(X_i), \\ var\left(\prod_{i=1}^{n} X_i\right) &= \prod_{i=1}^{n} \left[avg^2(X_i) + var(X_i)\right] - \prod_{i=1}^{n} avg^2(X_i). \end{aligned}$$

Thus they can be rewritten more usefully as:

$$\begin{aligned} avg\left[\chi_L^d\right] &= 2^d \cdot \prod_{i=0}^{d-1}(L-i), \\ var\left[\chi_L^d\right] &= \prod_{i=0}^{d-1} 4(L-i)(L-i+1) - \prod_{i=0}^{d-1} 4(L-i)^2, \\ avg\left[\Lambda_L^d\right] &= d \cdot \ln 2 + \sum_{i=0}^{d-1} \psi^0(L-i), \\ var\left[\Lambda_L^d\right] &= \sum_{i=0}^{d-1} \psi^1(L-i) \end{aligned}$$

APPENDIX B
DERIVING THE CHARACTERISTIC FUNCTIONS FOR THE CONSISTENT MEASURES OF DISTANCE

Given that the characteristic function (CF) of the elementary log-chi square distributions can be written as

$$CF_{\Lambda(2L)}(t) = 2^{it}\Gamma(L+it)/\Gamma(L)$$

then the CF for the following random variables, which are combinations of the above elementary random variables, can be derived

$$\begin{aligned}
\Lambda_L^d &\sim \sum_{i=0}^{d-1} \Lambda(2L-2i) \\
\mathbb{L} &\sim \Lambda_L^d - d \cdot \ln(2L) \\
\mathbb{D} &\sim \mathbb{L} - d \cdot \ln L + \sum_{i=0}^{d-1} \psi^0(L-i) \\
\mathbb{C} &\sim \sum_{i=0}^{d-1} [\Lambda(2L-2i) - \Lambda(2L-2i)]
\end{aligned}$$

Since we can state that

$$\begin{aligned}
CF_{\sum X_i}(t) &= \prod CF_{X_i}(t) \\
CF_{x+k}(t) &= e^{itk} CF_x(t)
\end{aligned}$$

then we have:

$$CF_{\Lambda_L^d}(t) = \frac{2^{idt}}{\Gamma(L)^d} \prod_{j=0}^{d-1} \Gamma(L-j+it) \tag{B.19}$$

$$CF_{\mathbb{L}} = \frac{1}{L^{idt}\Gamma(L)^d} \prod_{j=0}^{d-1} \Gamma(L-j+it) \tag{B.20}$$

$$CF_{\mathbb{D}} = \frac{1}{\Gamma(L)^d} \prod_{j=0}^{d-1} e^{idt\psi^0(L-j)} \Gamma(L-j+it) \tag{B.21}$$

Also due to

$$\begin{aligned}
CF_{-\Lambda(2L)}(t) &= 2^{-it} \frac{\Gamma(L-it)}{\Gamma(L)} \\
\Delta(2L) &\sim \Lambda(2L) - \Lambda(2L) \\
\Gamma(L-it)\Gamma(L+it) &= \Gamma(2L) B(L-it, L+it) \\
CF_{\Delta(2L)}(t) &= \frac{\Gamma(2L) B(L-it, L+it)}{\Gamma^2(L)}
\end{aligned}$$

then we arrive at:

$$CF_{\mathbb{C}} = \prod_{j=0}^{d-1} \frac{\Gamma(2L-2j) B(L-j-it, L-j+it)}{\Gamma^2(L-j)} \tag{B.22}$$

with $\Gamma()$ and $B()$ denoting Gamma and Beta functions respectively.

APPENDIX C
SAR INTENSITY AS A SPECIAL CASE OF POLSAR COVARIANCE MATRIX DETERMINANT

In this appendix, the following results for SAR intensity I are shown to be special cases of the results given in this paper for the determinant of the POLSAR covariance matrix $det|C_v|$. Specifically, the following results extend from the authors previous work on single-look SAR [17], i.e. $d = L = 1$, which is considerd a special case. We can state the following:

$$I \sim \bar{I} \cdot pdf\left[e^{-R}\right] \tag{C.23}$$

$$\log_2 I \sim \log_2 \bar{I} + pdf\left[2^{D-2^D}\right] \tag{C.24}$$

$$\frac{I}{\bar{I}} = \mathbb{R} \sim pdf\left[e^{-R}\right] \tag{C.25}$$

$$\log_2 I - \log_2 \bar{I} = \mathbb{D} \sim pdf\left[2^D e^{-2^D} \ln 2\right] \tag{C.26}$$

$$\log_2 I_1 - \log_2 I_2 = \mathbb{C} \sim pdf\left[\frac{2^c}{(1+2^c)^2} \ln 2\right] \tag{C.27}$$

$$avg(\mathbb{D}) = -\gamma / \ln 2 \tag{C.28}$$

$$var(\mathbb{D}) = \frac{\pi^2}{6}\frac{1}{\ln^2 2} \tag{C.29}$$

$$mse(\mathbb{D}) = \frac{1}{\ln^2 2}(\gamma^2 + \pi^2/6) = 4.1161 \tag{C.30}$$

but also the following well-known results are considered for multi-look SAR, i.e. $d = 1, L > 1$:

$$I \sim pdf\left[\frac{L^L I^{L-1} e^{-LI/\bar{I}}}{\Gamma(L)\bar{I}^L}\right] \tag{C.31}$$

$$N = \ln I \sim pdf\left[\frac{L^L}{\Gamma(L)} e^{L(N-\bar{N})-Le^{N-\bar{N}}}\right] \tag{C.32}$$

It will be shown that all of these results are special cases of the result derived previously and rewritten below:

$$|C_v| \sim \frac{|\Sigma_v|}{(2L)^d} \prod_{i=0}^{d-1} \chi^2(2L-2i) \tag{C.33}$$

$$\ln|C_v| \sim \ln|\Sigma_v| + \sum_{i=0}^{d-1} \Lambda(2L-2i) - d \cdot \ln 2L \tag{C.34}$$

$$\frac{|C_v|}{|\Sigma_v|} = \mathbb{R} \sim \frac{1}{(2L)^d}\prod_{i=0}^{d-1}\chi^2(2L-2i) \tag{C.35}$$

$$\ln|C_v| - \ln|\Sigma_v| = \mathbb{D} \sim \sum_{i=0}^{d-1}\Lambda(2L-2i) - d\cdot\ln 2L \tag{C.36}$$

$$\ln|C_{1v}| - \ln|C_{2v}| = \mathbb{C} \sim \sum_{i=0}^{d-1}\Delta(2L-2i) \tag{C.37}$$

$$avg(\mathbb{D}) = \sum_{i=0}^{d-1}\psi^0(L-i) - d\cdot\ln L \tag{C.38}$$

$$var(\mathbb{D}) = \sum_{i=0}^{d-1}\psi^1(L-i) \tag{C.39}$$

$$mse(\mathbb{D}) = \left[\sum_{i=0}^{d-1}\psi^0(L-i) - d\cdot\ln L\right]^2 + \sum_{i=0}^{d-1}\psi^1(L-i) \tag{C.40}$$

This appendix also derives new results for multi-look SAR data, which can be thought of either as extensions of the corresponding single-look SAR results or as simple cases of the POLSAR results presented above. They are:

$$\frac{I}{\bar{I}} = \mathbb{R} \sim \frac{1}{2L}\chi^2(2L) \tag{C.41}$$

$$\ln I - \ln\bar{I} = \mathbb{D} \sim \Lambda(2L) - \ln 2L \tag{C.42}$$

$$\ln I_1 - \ln I_2 = \mathbb{C} \sim \Delta(2L) \tag{C.43}$$

$$avg(\mathbb{D}) = \psi^0(L) - \ln L \tag{C.44}$$

$$var(\mathbb{D}) = \psi^1(L) \tag{C.45}$$

$$mse(\mathbb{D}) = \left[\psi^0(L) - \ln L\right]^2 + \psi^1(L) \tag{C.46}$$

The derivation process detailed below consists of two-phases. The first phase collapses the generic multi-dimensional POLSAR results into the classical one-dimensional SAR domain. Mathematically this means setting the dimensional number in POLSAR to $d = 1$ and collapsing the POLSAR covariance matrix into the variance measure in SAR, which also equals the SAR intensity i.e. $|C_v| = I, |\Sigma_v| = \bar{I}$.

The output of the first phase, in the general case, is applicable to multi-look SAR data, where $d = 1$ but $L > 1$. The second phase simplifies the multi-look results into single-look results,

which will match those presented in our previous work [17]. Mathematically, it means setting $L = 1$ in the multi-look result and converting from the natural logarithmic domain used in this paper to the base-2 logarithm used in [17] (base-2 was chosen in the previous paper to simplify the computation).

A. Original Domain: SAR Intensity and its ratio

Setting $d = 1$, $|C_v| = I$ and $|\Sigma_v| = \bar{I}$ into Eqns. C.33 and C.35 we find that:

$$\begin{aligned} I &\sim \frac{\bar{I}}{2L}\chi^2(2L) \\ \frac{I}{\bar{I}} = \mathbb{R} &\sim \frac{1}{2L}\chi^2(2L) \end{aligned}$$

Or in PDF forms, and applying the variable change theorem,:

$$\begin{aligned} \frac{2LI}{\bar{I}} &\sim pdf\left[\frac{x^{L-1}e^{-x/2}}{2^L\Gamma(L)}\right] \\ \frac{I}{\bar{I}} &\sim pdf\left[\frac{x^{L-1}e^{-x/2}}{2^L\Gamma(L)}\cdot dx/dt\right]_{x=2L\cdot t} \\ &\sim pdf\left[\frac{L^L t^{L-1}e^{-Lt}}{\Gamma(L)}\right] \\ I &\sim pdf\left[\frac{L^L t^{L-1}e^{-Lt}}{\Gamma(L)}\cdot dt/dx\right]_{t=x/\bar{I}} \\ &\sim pdf\left[\frac{L^L x^{L-1}e^{-Lx/\bar{I}}}{\bar{I}^L\Gamma(L)}\right] \end{aligned}$$

Thus we have the following results for multi-look SAR:

$$I \sim pdf\left[\frac{L^L x^{L-1}e^{-Lx/\bar{x}}}{\bar{I}^L\Gamma(L)}\right] \tag{C.47}$$

$$\frac{I}{\bar{I}} = \mathbb{R} \sim pdf\left[\frac{L^L x^{L-1}e^{-Lx}}{\Gamma(L)}\right] \tag{C.48}$$

Now setting $L = 1$, these results become:

$$I \sim pdf\left[\frac{e^{x/\bar{I}}}{\bar{I}}\right] \tag{C.49}$$

$$\frac{I}{\bar{I}} = \mathbb{R} \sim pdf\left[e^{-x}\right] \tag{C.50}$$

which is the same as stated in [17], demonstrating that the previous work is a special case of the more generic POLSAR forms.

B. Log-transformed domain: SAR log-intensity and the log-distance

The result for multi-look SAR data written in the log-transformed domain can be derived from two different approaches. The first is to follow a simplification method, where the results for log-transformed POLSAR data are simplified into log-transformed multi-look SAR results.

The second approach is to apply log-transformation to the results derived in the previous section. In this section, it is shown that both approaches would result in identical results.

Setting $d = 1$, $|C_v| = I$ and $|\Sigma_v| = \bar{I}$ into Eqns. C.34 and C.36 we have

$$\begin{aligned} \ln I &\sim \ln \bar{I} + \Lambda(2L) - \ln 2L \\ \ln I - \ln \bar{I} = \mathbb{L} &\sim \Lambda(2L) - \ln 2L \end{aligned}$$

Or in PDF form, and applying the variable change theorem we have:

$$\begin{aligned} \ln I - \ln \bar{I} + \ln 2L &\sim pdf\left[\frac{e^{Lx-e^x/2}}{2^L\Gamma(L)}\right] \\ \ln I - \ln \bar{I} &\sim pdf\left[\frac{e^{Lx-e^x/2}}{2^L\Gamma(L)} \cdot dx/dt\right]_{x=t+\ln 2L} \\ &\sim pdf\left[\frac{L^L e^{Lt-Le^t}}{\Gamma(L)}\right] \\ \ln I &\sim pdf\left[\frac{L^L e^{Lt-Le^t}}{\Gamma(L)} \cdot dt/dx\right]_{t=x-\ln \bar{I}} \\ &\sim pdf\left[\frac{L^L e^{L(x-\bar{N})-Le^{x-\bar{N}}}}{\Gamma(L)}\right] \end{aligned}$$

with $\bar{N} = \ln \bar{I}$. Thus the first approach arrives at

$$\ln I = \mathbb{N} \sim pdf\left[\frac{L^L e^{L(x-\bar{N})-Le^{x-\bar{N}}}}{\Gamma(L)}\right] \tag{C.51}$$

$$\ln I - \ln \bar{I} = \mathbb{L} \sim pdf\left[\frac{L^L e^{Lt-Le^t}}{\Gamma(L)}\right] \tag{C.52}$$

In the second approach, log-transformation is applied on previous results for multi-look SAR intensity and its ratio in the original domain (Eqns. C.48 and C.47). This also arrives at the same results shown above, however the detailed working is omitted for brevity.

To compute summary statistics for the multi-look SAR dispersion, set $d = 1$ into Eqns. C.40, C.38 and C.39 we have:

$$\begin{aligned} avg(\mathbb{L}) &= \psi^0(L) - \ln L \\ var(\mathbb{L}) &= \psi^1(L) \\ mse(\mathbb{L}) &= \left[\psi^0(L) - \ln L\right]^2 + \psi^1(L) \end{aligned}$$

This completes the first phase of the derivation process. The second phase of simplification involves setting $L = 1$ into the above results for multi-look SAR data, and converting natural logarithm into base-2 logarithm. First, setting $L = 1$ makes the above results become

$$\begin{aligned} \ln I = \mathbb{N} &\sim pdf\left[e^{(x-\bar{N})-e^{x-\bar{N}}}\right] \\ \ln I - \ln \bar{I} = \mathbb{L} &\sim pdf\left[e^{x-e^x}\right] \\ avg(\mathbb{L}) &= \psi^0(1) = -\gamma \\ var(\mathbb{L}) &= \psi^1(1) = \pi^2/6 \\ mse(\mathbb{L}) &= \left[\psi^0(1)\right]^2 + \psi^1(1) = \gamma^2 + \pi^2/6 \end{aligned}$$

with γ denoting the Euler-Mascharoni constant. Then to convert to base-2 logarithm from natural logarithmic transformation, we again use the variable change theorem. That is:

$$\begin{aligned} \log_2 I = \mathbb{N}_2 &\sim pdf\left[e^{(x-\bar{N})-e^{x-\bar{N}}} \cdot dx/dt\right]_{x=t\cdot\ln 2} \\ \mathbb{N}/\ln 2 = \mathbb{N}_2 &\sim pdf\left[e^{(t\cdot\ln 2-\bar{N})-e^{t\cdot\ln 2-\bar{N}}} \ln 2\right]_{\bar{N}_2=\bar{N}\cdot\ln 2} \\ &\sim pdf\left[2^{t-\bar{N}_2} e^{2^{t-\bar{N}_2}} \ln 2\right] \end{aligned}$$

$$\begin{aligned} \log_2 I - \log_2 \bar{I} = \mathbb{L}/\ln 2 = \mathbb{L}_2 &\sim pdf\left[e^{x-e^x}\right]_{x=t\cdot\ln 2} \\ &\sim pdf\left[2^t e^{2^t} \ln 2\right] \end{aligned}$$

$$\begin{aligned} avg(\mathbb{L}_2) &= avg(\mathbb{L})/\ln 2 = -\gamma/\ln 2 \\ var(\mathbb{L}_2) &= var(\mathbb{L})/\ln^2 2 = \frac{\pi^2}{6}\frac{1}{\ln^2 2} \\ mse(\mathbb{L}_2) &= mse(\mathbb{L})/\ln^2 2 = \frac{1}{\ln^2 2}(\gamma^2 + \pi^2/6) = 4.1161 \end{aligned}$$

C. Deriving the PDF for SAR dispersion and contrast

The PDF for SAR dispersion can be easily derived from the PDF for the log-distance given above as:

$$\ln I - avg(\ln I) = \mathbb{D} \sim pdf\left[\frac{e^{L[x+\psi^0(L)]-Le^{x+\psi^0(L)-\ln L}}}{\Gamma(L)}\right] \tag{C.53}$$

due to $d = 1$ and

$$\begin{aligned} \mathbb{D} &\sim \mathbb{L} - avg(\mathbb{L}) \\ avg(\mathbb{L}) &= \psi^0(L) - \ln L \\ \mathbb{L} &\sim pdf\left[\frac{L^L e^{Lt-Le^t}}{\Gamma(L)}\right] \end{aligned}$$

Setting $L = 1$ for Single-Look SAR we have

$$\mathbb{D} \sim pdf\left[e^{x-\gamma-e^{x-\gamma}}\right] \tag{C.54}$$

due to: $\psi^0(1) = -\gamma$ and $\Gamma(1) = 1$ with γ being the Euler Mascheroni constant (which equals 0.5772). In base-2 logarithm domain, invoking the variable change theorem:

$$\begin{aligned} \mathbb{D}_2 &= \log_2 I - avg(\log_2 I) = \mathbb{D}/\ln 2 \\ \mathbb{D}_2 &\sim pdf\left[e^{x-\gamma-e^{x-\gamma}} \cdot \frac{dx}{dt}\right]_{x=t\cdot\ln 2} \end{aligned}$$

Thus we have

$$\mathbb{D}_2 \sim pdf\left[e^{-(2^x e^{-\gamma})}(2^x e^{-\gamma})\ln 2\right] \tag{C.55}$$

which is consistent with the results found in our previous work [17].

Setting $d = 1$ into Eqn. for contrast results in

$$\ln I_1 - \ln I_2 = \mathbb{C} \sim \Delta(2L) \tag{C.56}$$

The characteristic function would then be

$$CF_{\mathbb{C}} = \frac{\Gamma(2L)B(L-it, L+it)}{\Gamma(L)^2} \tag{C.57}$$

Thus the PDF can be written as

$$\mathbb{C} \sim pdf\left[\frac{\Gamma(2L)}{\Gamma(L)^2}\frac{e^{Lx}}{(1+e^x)^{2L}}\right] \tag{C.58}$$

due to

$$\begin{aligned} CF_{\mathbb{C}}(x) &= \frac{\Gamma(2L)}{\Gamma(L)^2} B(1/(1+e^x), L-it, L+it) \\ &= \frac{\Gamma(2L)}{\Gamma(L)^2} \int_0^{1/(1+e^x)} z^{L-it-1}(1-z)^{L+it-1} dz \\ \frac{\partial}{\partial x} CF_{\mathbb{C}}(x) &= \frac{\partial CF_{\mathbb{C}}(x)}{\partial 1/(1+e^x)} \cdot \frac{\partial 1/(1+e^x)}{\partial x} \\ &= e^{itx} \frac{\Gamma(2L)}{\Gamma(L)^2} \frac{e^{Lx}}{(1+e^x)^{2L}} \end{aligned}$$

Setting $L = 1$ into Eqn. C.58 we have the PDF for contrast of single-look SAR data:

$$\mathbb{C} \sim pdf\left[\frac{e^x}{(1+e^x)^2}\right] \tag{C.59}$$

Converting to base-2 logarithm gives the following:

$$\begin{aligned} \mathbb{C}/\ln 2 = \mathbb{C}_2 &\sim pdf\left[\frac{e^x}{(1+e^x)^2} \cdot dx/dt\right]_{x=t\cdot\ln 2} \\ &\sim pdf\left[\ln 2 \frac{2^t}{(1+2^t)^2}\right] \end{aligned}$$

which is also consistent to the results shown in our previous work [17].

REFERENCES

[1] K. Conradsen, A. Nielsen, J. Schou, and H. Skriver, "A test statistic in the complex Wishart distribution and its application to change detection in polarimetric SAR data," *IEEE Transactions on Geoscience and Remote Sensing*, vol. 41, no. 1, pp. 4 – 19, Jan 2003.

[2] V. Alberga, G. Satalino, and D. K. Staykova, "Comparison of polarimetric sar observables in terms of classification performance," *International Journal of Remote Sensing*, vol. 29, no. 14, pp. 4129–4150, 2008. [Online]. Available: http://www.tandfonline.com/doi/abs/10.1080/01431160701840182

[3] I. Joughin, D. Winebrenner, and D. Percival, "Probability density functions for multilook polarimetric signatures," *Geoscience and Remote Sensing, IEEE Transactions on*, vol. 32, no. 3, pp. 562 –574, may 1994.

[4] J.-S. Lee, K. Hoppel, S. Mango, and A. Miller, "Intensity and phase statistics of multilook polarimetric and interferometric SAR imagery," *IEEE Transactions on Geoscience and Remote Sensing*, vol. 32, no. 5, pp. 1017 –1028, Sep 1994.

[5] R. Touzi and A. Lopes, "Statistics of the stokes parameters and of the complex coherence parameters in one-look and multilook speckle fields," *Geoscience and Remote Sensing, IEEE Transactions on*, vol. 34, no. 2, pp. 519 –531, mar 1996.

[6] C. Lopez-Martinez and X. Fabregas, "Polarimetric sar speckle noise model," *Geoscience and Remote Sensing, IEEE Transactions on*, vol. 41, no. 10, pp. 2232–2242, 2003.

[7] E. Erten, "The performance analysis based on SAR sample covariance matrix," *Sensors (Basel)*, vol. 12, no. 3, pp. 2766–2786, 2012.

[8] M. Dabboor, J. Yackel, M. Hossain, and A. Braun, "Comparing matrix distance measures for unsupervised POLSAR data classification of sea ice based on agglomerative clustering," *International Journal of Remote Sensing*, vol. 34, no. 4, pp. 1492–1505, 2013.

[9] P. Kersten, J. S. Lee, and T. Ainsworth, "Unsupervised classification of polarimetric synthetic aperture radar images using fuzzy clustering and EM clustering," *IEEE Transactions on Geoscience and Remote Sensing*, vol. 43, no. 3, pp. 519 – 527, Mar 2005.

[10] J.-S. Lee, M. Grunes, and G. de Grandi, "Polarimetric SAR speckle filtering and its implication for classification," *IEEE Transactions on Geoscience and Remote Sensing*, vol. 37, no. 5, pp. 2363 –2373, Sep 1999.

[11] J. S. Lee, M. R. Grunes, and R. Kwok, "Classification of multi-look polarimetric SAR imagery based on complex Wishart distribution," *International Journal of Remote Sensing*, vol. 15, no. 11, pp. 2299–2311, 1994.

[12] S. N. Anfinsen, R. Jenssen, and T. Eltoft, "Spectral clustering of polarimetric SAR data with Wishart-derived distance measures," in *3rd International Workshop on Science and Applications of SAR Polarimetry and Polarimetric Interferometry*, vol. 3, Jan 2007.

[13] K. Y. Lee and T. Bretschneider, "Derivation of separability measures based on central complex Gaussian and Wishart distributions," in *IEEE Internationaal Geoscience and Remote Sensing Symposium (IGARSS), 2011*, Jul 2011, pp. 3740 –3743.

[14] F. Cao, W. Hong, Y. Wu, and E. Pottier, "An unsupervised segmentation with an adaptive number of clusters using the SPAN/H/α/A space and the complex Wishart clustering for fully polarimetric SAR data analysis," *IEEE Transactions on Geoscience and Remote Sensing*, vol. 45, no. 11, pp. 3454 –3467, Nov 2007.

[15] N. R. Goodman, "The distribution of the determinant of a complex Wishart distributed matrix," *Annals of Mathematical Statistics*, vol. 34, no. 1, pp. 178–180, 1963.

[16] T. H. Le, I. V. McLoughlin, K. Y. Lee, and T. Brestchneider, "SLC SAR speckle filtering using homoskedastic features of logarithmic transformation," in *Proceedings of the 31th Asian Conference on Remote Sensing (ACRS)*, Hanoi, Vietnam, Nov 2010.

[17] T. H. Le, I. V. McLoughlin, Q. H. Nguyen, and C. H. Vun, "Using MSE to evaluate SAR speckle filters," *IEEE Transactions on Geoscience and Remote Sensing*, vol. ??, no. ??, pp. ??? –???, ??? 2013, (Work-In-Progress).

[18] R. Raney and G. Wessels, "Spatial considerations in SAR speckle consideration," *IEEE Transactions on Geoscience and Remote Sensing*, vol. 26, no. 5, pp. 666 –672, Sep 1988.

[19] S. Anfinsen, A. Doulgeris, and T. Eltoft, "Estimation of the equivalent number of looks in polarimetric synthetic aperture radar imagery," *IEEE Transactions on Geoscience and Remote Sensing*, vol. 47, no. 11, pp. 3795 –3809, Nov 2009.

[20] "AIRSAR implementation," [Accessed Feb 2013]. [Online]. Available: http://airsar.jpl.nasa.gov/documents/genairsar/chapter3.pdf

[21] "RadarSat-2 product description," [Accessed Feb 2013]. [Online]. Available: http://gs.mdacorporation.com/products/sensor/radarsat2/RS2_Product_Description.pdf

[22] A. Freeman and S. Durden, "A three-component scattering model for polarimetric SAR data," *IEEE Transactions on Geoscience and Remote Sensing*, vol. 36, no. 3, pp. 963 –973, May 1998.

[23] S. Cloude and E. Pottier, "An entropy based classification scheme for land applications of polarimetric SAR," *IEEE Transactions on Geoscience and Remote Sensing*, vol. 35, no. 1, pp. 68 –78, Jan 1997.

[24] J. Schou, H. Skriver, A. Nielsen, and K. Conradsen, "CFAR edge detector for polarimetric SAR images," *IEEE Transactions on Geoscience and Remote Sensing*, vol. 41, no. 1, pp. 20 – 32, Jan 2003.

[25] T. H. Le and I. V. McLoughlin, "SAR Fuzzy-MLE speckle filter using the distance consistency property in homoskedastic log-transformed domain," in *Proceedings of the 32th Asian Conference on Remote Sensing (ACRS)*, Taipei, Taiwan, Nov 2011.

[26] F. Medeiros, N. Mascarenhas, and L. Costa, "Evaluation of speckle noise MAP filtering algorithms applied to SAR images," *International Journal of Remote Sensing*, vol. 24, no. 24, pp. 5197–5218, Dec 2003.